Physics AUC, vol. 21, 101-113 (2011)

Mapping models for magnetic configurations in tokamaks

D. Constantinescu[1] and M-C Firpo[2]
[1]*Dept. of Applied Math., Faculty of Exact Sciences, University of Craiova, Craiova 200585, Romania*
[2]*Laboratoire de Physique des Plasmas, CNRS, Ecole Polytechnique, 91128 Palaiseau Cedex, France*

Abstract

This paper is devoted to the study of some mapping models for the study of magnetic configurations in tokamaks which exhibit non-axisymmetric MHD or RMP perturbations. The destruction of a transport barrier is described using the transmissivity between the chaotic zones situated of its both sides.

1 Introduction

Many important models in astronomy, plasma physics, fluid dynamics and mechanics are one-degree-of-freedom Hamiltonian systems subjected to time periodic perturbations. Such models, corresponding to specific Hamiltonians and interpretation of action-angle variables, are successfully used for the study of transport and mixing in the ocean and atmosphere [1]-[2], of chaotic ray propagation in deep sea [3],of propagation of the pressure waves in pulsating stars of low mass [4], of magnetic configurations of hot plasma physics devices, such as tokamaks [5]-[7] etc.

In their study, a special attention was given to the existence of invariant surfaces (tori) because they can not be crossed by the orbits of the system, so they act as barriers which separate invariant zones of the space. In the unperturbed system every orbit lives on an invariant torus and the dynamics of the (integrable) system is regular. The complicate dynamics of the perturbed systems is partially due to the destruction of the barriers, which enables the orbit to wander in a larger zone of the phase space. This separation is very important in many phenomena: for transport and mixing in the ocean and atmosphere, these barriers give rise to the creation of 'ozone holes' since they isolate the ozone created in the tropics from Earth's polar regions [1]-[2], the chaotic ray propagation in deep sea and the propagation of the pressure waves in pulsating stars of low mass are also prevented by the existence of a transport barrier [3]-[4]. In magnetic confinement fusion, the existence of internal transport barriers in the magnetic configurations of hot plasma physics devices, such as tokamaks, may be viewed as a fundamental prerequisite for the confinement of charged particles.

The Hamiltonian, written in action-angle variables (θ, I) is $H : S^1 \times D \times [0, \infty) \to \mathbf{R}$

$$H(\theta, I, t) = H_0(I) + \varepsilon \cdot H_{pert}(\theta, I, t) \tag{1}$$

where S^1 denotes the circle $\mathbf{R}/(2\pi\mathbf{Z})$, $D \subset \mathbf{R}$ is the definition domain of the action variable I, and $H_{pert}(\theta, I, t) = H_{pert}(\theta, I, t+T)$ for a given time period $T \in \mathbf{R}_+$for all $t \in [0, \infty)$.

The associated Hamiltonian system is

$$\begin{cases} \frac{\partial \theta}{\partial t} = H_0'(I) + \varepsilon \cdot \frac{\partial H_{pert}}{\partial I} \\ \frac{\partial I}{\partial t} = -\frac{\partial H_{pert}}{\partial \theta} \end{cases} \tag{2}$$

The systems (2), known as $1\frac{1}{2}$ degrees of freedom Hamiltonian systems, are generically non-integrable. Their typical dynamics is not entirely regular (periodic orbits or quasi-periodic orbits lying on invariant tori) nor entirely chaotic (the chaotic orbits densely fill regions with positive measure in the phase space but not the whole space). Both dynamical regimes are connected in a complicate layer where regular and chaotic motion can not mix.

It is widely accepted that the essential aspects of the dynamics of such system are captured by the discrete dynamical system generated by the stroboscopic map with the stroboscopic time, i.e. the shift operator by time T, $SM_\varepsilon : S^1 \times D \to S^1 \times \mathbf{R}$

$$SM_\varepsilon(\theta(0), I(0)) = (\theta(T), I(T))$$

It generates a two dimensional discrete dynamical system

$$(\theta_{n+1}, I_{n+1}) = SM_\varepsilon(\theta_n, I_n)$$

where $(\theta_n, I_n) = (\theta(nT), I(nT))$. The discrete orbit of $(\theta_0, I_0) = (\theta(0).I(0))$ is obtained by recording the coordinates of its trajectory at times T, $2T$, $3T$,...

In [7] it is shown that the stroboscopic map is a particular case of Poincaré map, adapted to the particular characteristics of $1\frac{1}{2}$ degrees of freedom Hamiltonian systems with periodic perturbation. In this way, the complex behavior of $1\frac{1}{2}$ degrees of freedom Hamiltonian systems can be understood by studying area preserving maps, which are relatively simpler mathematical objects than differential equations.

The aim of this paper is to study some realistic magnetic configurations in tokamaks using discrete Hamiltonian models obtained by mapping techniques which are based on Hamilton-Jacobi theory. In this case the equations of the magnetic field lines can be cast in Hamiltonian form (2), where the action is the toroidal magnetic flux ψ conjugated to the polar angle θ and the toroidal angle ζ plays the role of time. The Hamiltonian H is the poloidal magnetic flux and $H_0'(\psi) \overset{notation}{=} W(\psi)$ is the winding function, the inverse of the safety factor $q(\psi)$. The term $\varepsilon \cdot H_{pert}(\theta, \psi, \zeta)$ describes the effect of magnetic perturbations. In our study we focus on the description of the chaotic dynamics and on the formation/destruction of the internal transport barriers because the existence of magnetic transport barriers is essential in the confinement of plasma (it prevents the large radial displacement of the charged particles).

The paper is structured as follows: in Section 2 the mapping techniques are described ; two models of the magnetic field lines in tokamaks are obtained in Section 3; Section 4 is devoted to the study of the model corresponding to MHD perturbations and the results are summarized in Section 5.

2 General mapping models

The exact Poincare map can not be always analytically determined because this is equivalent to solving analytically the system. Usually it is approximated using various techniques. There are two philosophically different ways to obtain approximations of the stroboscopic map: by performing a numerical integration with small step or by using the mapping techniques with large step.

In order to obtain a correct approximation of the stroboscopic map by numerical integration one must use a symplectic integrator, because the standard numerical methods introduce non-Hamiltonian perturbations that lead to a completely different long-time behavior [8]. The main goal of mapping models is to replace the Poincare maps of the original system by iterative maps. The maps are constructed in the symplectic form, hence they preserve the most important property of the original system. They run much faster than the small step numerical integration, but the main advantage is that the mapping models have better accuracy in the study of the chaotic dynamics due to the fact that the accumulation of the round-off errors is reduced. The general mapping technique used for obtaining good approximations of the stroboscopic map is based on the Hamilton-Jacobi method [9].

For the Hamiltonian, having time-periodic perturbation with the period 2π,

$$H(\theta, I, t) = H_0(I) + \sum_{m,n} \varepsilon_{mn} \cdot H_{mn}(I) \cos(m\theta - nt)$$

the Hamilton-Jacobi map, with the step $\Delta t = \frac{2\pi}{k}$ is (see [9]):

$$HJ : [0, 2\pi) \times [0, \infty) \times [0, 2\pi) \to [0, 2\pi) \times [0, \infty) \times [0, 2\pi)$$

given by:

$$HJ : \begin{cases} \overline{t} = t + 2\pi/k \\ \overline{\theta} = \left(\theta + \frac{2\pi}{k} \cdot W(X) + \varepsilon \frac{\partial S}{\partial X}(\theta, X, t) + \varepsilon \frac{\partial S}{\partial X}\left(\overline{\theta}, X, \overline{t}\right)\right) (\mathrm{mod}\, 2\pi) \\ \overline{I} = I - \varepsilon \frac{\partial S}{\partial \theta}(\theta, X, t) - \varepsilon \frac{\partial S}{\partial \overline{\theta}}\left(\overline{\theta}, X, \overline{t}\right) \end{cases} \tag{3}$$

where X is the (unique) solution of the equation

$$X = I - \varepsilon \frac{\partial S}{\partial \theta}(\theta, X, t). \tag{4}$$

The generating function S , involved in (3),(4), is defined by

$$S(\theta, X, t) = \frac{\pi}{k} \sum_{m,n} H_{m,n}(I) \left[a(x_{mn}) \sin(m\theta - nt) + b(x_{mn}) \cos(m\theta - nt)\right] \tag{5}$$

where

$$a(x) = \frac{1 - \cos x}{x}; \qquad b(x) = \frac{\sin x}{x}, \quad x_{mn} = \frac{\pi}{k}(m \cdot W(X) - n). \tag{6}$$

In order to compute $HJ(\theta, \psi, \zeta)$ one must solve two (usually complicate) implicit equations: eq 4 and the second eq. in the system 3.

It is proved that HJ is a performing integrator, even if the integration step is quite large [9].

In this case, the Poincare map corresponding to a Poincare section $(S) : t = t_0$ is

$$PHJ : (S) \to (S), \quad PHJ(\theta, I) = \left(\underbrace{HJ \circ HJ \circ ... \circ HJ}_{k \quad times} \right)(\theta, I) \tag{7}$$

The Hamilton-Jacobi map may be used when n has a finite (small) number of natural values.

When the Hamiltonian perturbation is the sum of infinitely many term, i.e.

$$H(\theta, I, t\zeta) = H_0(I) + \varepsilon \sum_{m \in \mathbf{M}} H_m(I) \cos(m\theta) \sum_{s=-\infty}^{\infty} \cos(s \cdot Mn \cdot t)$$

where $\mathbf{M}$ is a finite set and $n \in \mathbf{N}$ is fixed, the Hamilton-Jacobi map has a simpler form, called the symmetric map (see [9]):

$$SM : [0, 2\pi) \times [0, \infty) \times [0, 2\pi) \to [0, 2\pi) \times [0, \infty) \times [0, 2\pi)$$

$$SM : \begin{cases} \overline{T} = \zeta + 2\pi / (M \cdot n) \\ \overline{\theta} = \theta + \frac{2\pi}{Mn} W(X) + \varepsilon \frac{\partial S}{\partial X}(\theta, X) + \varepsilon \frac{\partial S}{\partial X}(\overline{\theta}, X) \\ \overline{I} = I - \varepsilon \frac{\partial S}{\partial \theta}(\theta, X) - \varepsilon \frac{\partial S}{\partial \overline{\theta}}(\overline{\theta}, X) \end{cases} \tag{8}$$

where the generating function is

$$S(\theta, I) = \frac{\pi}{Mn} \sum_m H_m(I) \cos(m\theta) \tag{9}$$

and X is the (unique) solution of the implicit equation

$$X = I - \varepsilon \frac{\partial S}{\partial \theta}(\theta, X) \tag{10}$$

The mapping step is $\Delta t = \frac{2\pi}{Mn}$, so the Poincare map corresponding to a Poincare section $(S) : t = t_0$ is

$$PSM : (S) \to (S), \quad PSM(\theta, I) = \left(\underbrace{HJ \circ HJ \circ ... \circ HJ}_{Mn \quad times} \right)(\theta, I)$$

3 Magnetic maps

In order to describe some magnetic configurations that may be encountered in tokamaks (toroidal devices used for obtaining the thermo-controlled nuclear fusion) one can use the Hamiltonian description [7].

Because the tokamaks are toroidal devices, it is natural to use toroidal coordinates (r, θ, ζ)in order to describe the magnetic field (ζ is the toroidal angle and (r, θ) are the poloidal coordinates in a circular poloidal section). Instead of the poloidal radius r, the toroidal flux $\psi = r^2/2$ is commonly used because ψ and θ represent a pair of canonical variables [6].

The Hamiltonian system obtained from the equations of the magnetic field by using the Clebsh representation. The Hamiltonian of the system is the poloidal magnetic field

$$H(\theta, \psi, \zeta) = H_0(\psi) + \varepsilon \cdot H_{pert}(\theta, \psi, \zeta).$$

The unperturbed Hamiltonian, $H_0(\psi) = \int \frac{d\psi}{q(\psi)} = \int W(\psi)\, d\psi$, is the poloidal flux of the equilibrium plasma and the effect of magnetic perturbations is contained in the term $\varepsilon \cdot H_{pert}(\theta, \psi, \zeta)$.

In this case ψ represent the action variable and the toroidal angle ζ is interpreted in analogy with a "time variable".

The "time" section , $(S) : \zeta = \zeta_0$ is a vertical poloidal section of the device, i.e. $(S) = S^1 \times [0, \infty)$. The physical relevant interval for ψ is $[0, 1]$.

In this case, the mapping models (3)-(6) and (8)-(10) have an important physical interpretation: the pair (θ_n, ψ_n) indicates the re-intersection of the magnetic field line with (S) after toroidal n turns.

Realistic models requires knowledge of the safety factor and of the magnetic perturbations. Determination of these quantities from the experiment is a challenging task, because of the large uncertainties in the measurements.

3.1 The safety factor

The safety factor $q(r)$ is determined by the radial distribution of the plasma current density $j(r)$ while full radial, poloidal and toroidal values of $j(r, \theta, \zeta)$ are required for a precise knowledge of the magnetic topology. In experiments the safety factor can be derived from the observation of large striations observed during the ablation of injected hydrogen (deuterium) pellets [10].

The safety factor can be analytically obtained from the magneto-hydrodynamic theory [11], or from equilibrium code calculations, taking into account the position of the MHD modes identified in experiments.

In our examples we will use the safety factor derived in [11], namely

$$q(\psi) = \frac{4}{w(2-\psi)\left(2-2\psi+\psi^2\right)}; \tag{11}$$

For the safety factor (11) , with $w = 1$, the values of the main ψ_{mn} (where the modes (m, n) are situated in the unperturbed system) are:

$\psi_{4,3} = 0.189464$; $\psi_{2,1} = 0.456311$; $\psi_{5,2} = 0.610635$; $\psi_{3,1} = 0.746923$; $\psi_{7,2} = 0.874785$; $\psi_{11,3} = 0.916622$; $\psi_{15,4} = 0.937485$; $\psi_{19,5} = 0.949994$; $\psi_{23,6} = 0.958330$; $\psi_{27,7} = 0.964284$;

In Figure 1 the position of the main (m, n) modes is presented.

3.2 MHD perturbations

The magnetic perturbations are due to plasma instabilities (MHD-perturbations) or the addition of internal or external magnetic fields usually created by external applied electric currents (RMP- perturbations).

The MHD-perturbations (magnetohydrodynamic perturbations) corresponding to the (m, n) mode reads

$$\varepsilon_{mn} \cdot H_{mn}(\psi) \cos(m\theta - n\zeta + \chi_{mn})$$

where m, n are the poloidal and toroidal number, ε_{mn} and χ_{mn} are the amplitude and the phases of the (m, n)-MHD mode. The winding number is $W(\psi_{mn}) = n/m$, i.e. $q(\psi_{mn}) = m/n$ which means that the mode (m, n) is resonant at magnetic surface $\psi = \psi_{mn}$.

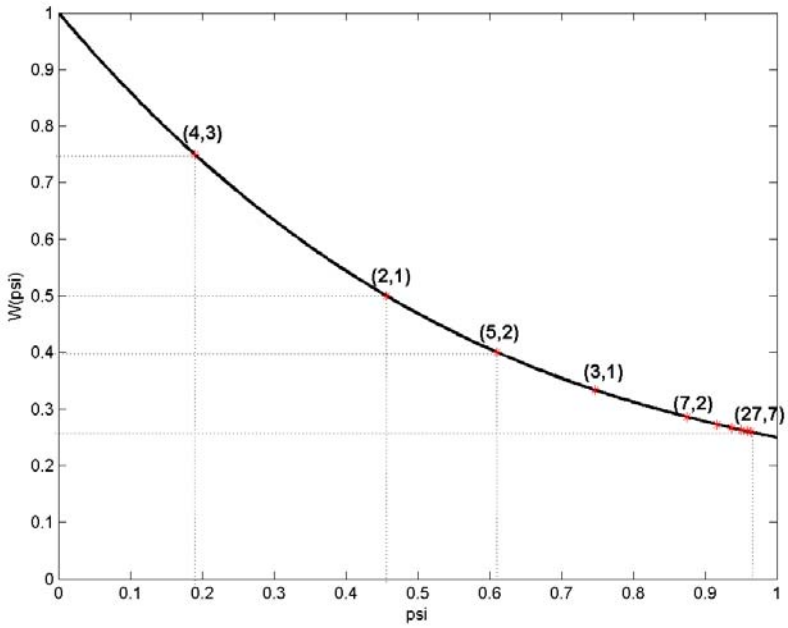

Figure 1: The position of the main (m,n) modes for the safety factor $q(\psi) = 4/\left((2-\psi)\left(2-2\psi+\psi^2\right)\right)$

In what follows we will use the MHD-perturbation proposed in [13]:

$$H_{mn} = \frac{n}{m}\left[\frac{(\psi/\psi_{mn})^{1/\Delta} + (\psi/\psi_{mn})^{-1/\Delta}}{2}\right]^{-m\Delta/2}. \tag{12}$$

The profile of MHD mode correctly describes the behavior near the resonant surfaces and it is in agreement with the parametrization proposed in [14], [12]

The MHD perturbations corresponding to $(4,3)$, $(7,2)$, $(27,7)$ can be seen in Figure 2

The internal magnetic perturbations which contains several (m,n) modes is

$$\varepsilon \cdot H_{pert}(\theta,\psi,\zeta) = \sum_{m,n} \varepsilon_{mn} \cdot H_{mn}(\psi)\cos(m\theta - n\zeta)$$

Remark 1 *In the Poincare section $\zeta = 0$, the perturbation $H_{mn}(\psi)\cdot\cos(m\theta)$ has local extrema in $(\theta,\psi) = \left(\frac{k\pi}{m}, \psi_{mn}\right)$, for $k \in \{0,1,...2m-1\}$*

The system generated by the Hamilton-Jacobi map (3), (4)-(6), corresponding to the safety factor (11) and the magnetic perturbations (12) and the step $\Delta\zeta = 2\pi$ will be called in the following sections "the MDH-model".

3.3 RMP-perturbations

There are also other important magnetic pertubations, namely those created by external saddle coils which are typically toroidally distributed inside or outside of a plasma vacuum vessel. The resonant magnetic perturbations (RMPs) created by these coils are non-axissymmetric along the poloidal and toroidal directions. Their effect is determined by

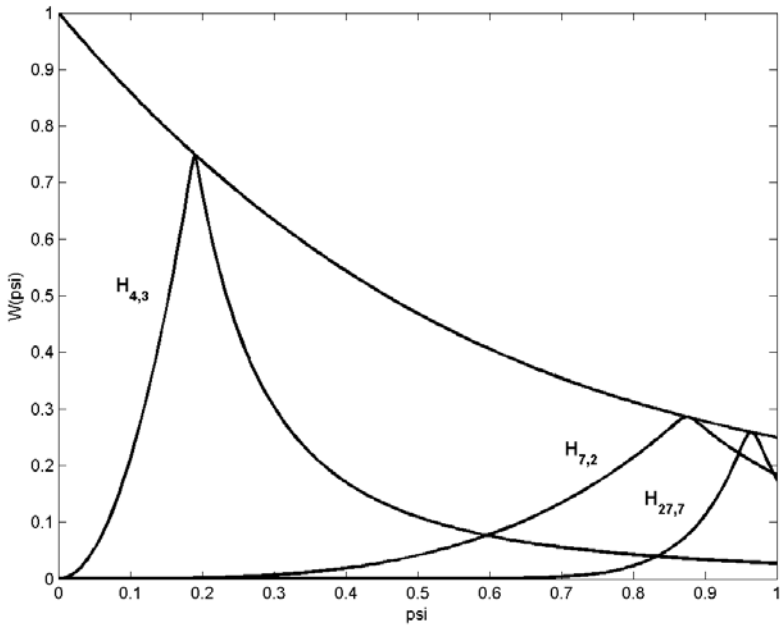

Figure 2: The MHD-perturbations corresponding to $(4,3)$, $(7,2)$, $(27,7)$.

the main (m,n) component of the Fourier expansion. For this reason, the saddle coils are designed to create a mode (m,n) with a fixed toroidal mode "n".

For fixed M, $n \in \mathbf{N}$, the general form of the perturbations having a broad spectrum near the separatrix is

$$\begin{aligned}\varepsilon \cdot H_{pert}(\theta,\psi,\zeta) &= \varepsilon \sum_m H_{mn}(\psi) \cos m\theta \sum_{s=-\infty}^{\infty} \cos(s \cdot Mn \cdot \zeta) \\ &= \varepsilon \sum_m H_{mn}(\psi) \sum_{s=0}^{\infty} \cos(m\theta - s \cdot Mn \cdot \zeta)\end{aligned}$$

. The simplest asymptotical form of H_{mn} was found using its relation with the generalized Poincare integral ([13], [15], [16]):

$$H_{mn}(\psi) = \frac{n}{m} e^{-m\frac{C(\psi)}{\gamma \cdot q(\psi)}}.$$

where $C(\psi)$ is an analytical function with a finite value in $\psi = 1$, which can be established from code calculations. In [13] $C(\psi)$ was chosen in the form

$$C(\psi) = C_0\psi - \frac{1}{2}\gamma \cdot q(\psi) \cdot \ln\psi$$

In this case we have

$$H_{mn}(\psi) = \frac{n}{m} \cdot \psi^{m/2} \cdot e^{-m \cdot C_0 \cdot \psi \cdot W(\psi)/\gamma} \tag{13}$$

depends on the constants C_0 and γ, which can be founded from the equilibrium calculations or from experiment (see [13]).

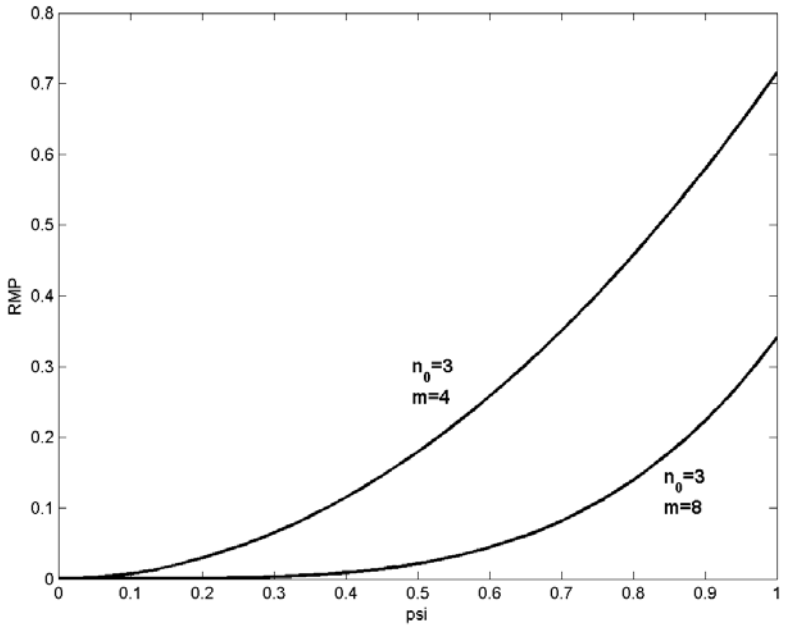

Figure 3: RMPs corresponding to $q(\psi) = 4/\left((2-\psi)\left(2-2\psi+\psi^2\right)\right)$ and $C_0 = 0.07$, $\gamma = 0.21$

Two RMP-perturbation, corresponding to the safety factor (11), $C_0 = 7\cdot 10^{-2}$, $\gamma = 0.21$ are drawn in Figure 3 .

The system generated by the symmetric map (8)-(10), corresponding to the safety factor (11) and the magnetic perturbations (13) and the step $\Delta\zeta = 2\pi$ will be called in the following sections "the RMP-model".

4 Stochasticity in MHD-model

In MHD model, even for very small amplitudes of more than one active MHD perturbation, one obtains chaotic behavior. This is due to the overlapping of stable and unstable manifolds of hyperbolic periodic points.

The perturbation corresponding to the simultaneous activation of $(2,1)$, $(5,2)$, $(3,1)$ and $(7,2)$ modes, with the amplitudes $\varepsilon_{2,1} = 0.003$, $\varepsilon_{5,2} = 0.001$, $\varepsilon_{3,1} = 0.002$ respectively $\varepsilon_{7,2} = 0.0005$ is presented in Figure 4.

The MHD-perturbation is symmetric to the line $\theta = \pi$ and its largest values are situated on the line $\theta = 0$.

In this case $\left|\sum_{m,n} \varepsilon_{m,n} H_{mn}(\psi)\cos(m\theta - n\zeta)\right| \leq 0.0026$, less than 0.7% of the unperturbed Hamiltonian, however the influence of MHD-perturbation on the configuration of magnetic field lines is remarkable.

In figure 5 is presented the phase-portrait of MHD-model where a chaotic dynamics is obtained through the activation of $(2,1)$, $(5,2)$, $(3,1)$ and $(7,2)$ modes. In the picture one can observe islands of two, five, three, respectively seven islands, corresponding to the excited modes.

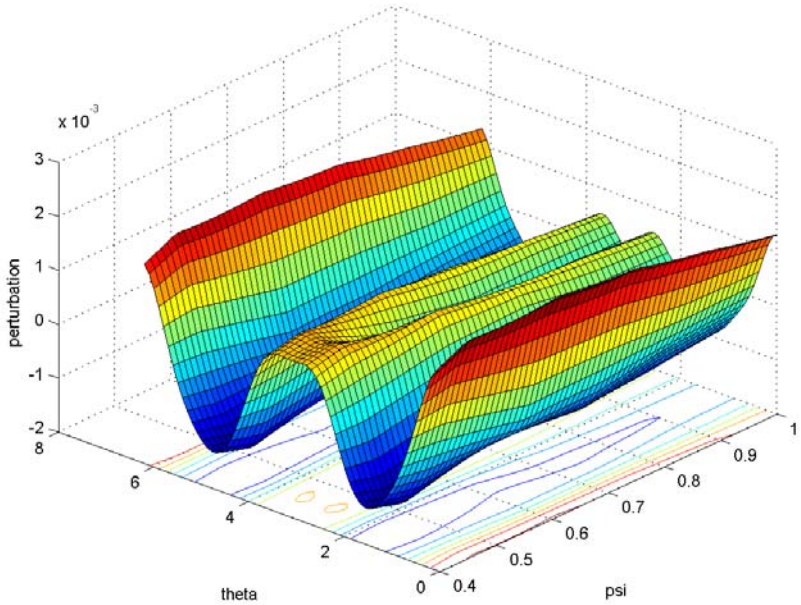

Figure 4: MHD perturbations when $(2,1)$, $(5,2)$, $(3,1)$ and $(7,2)$ modes are simultanous activated

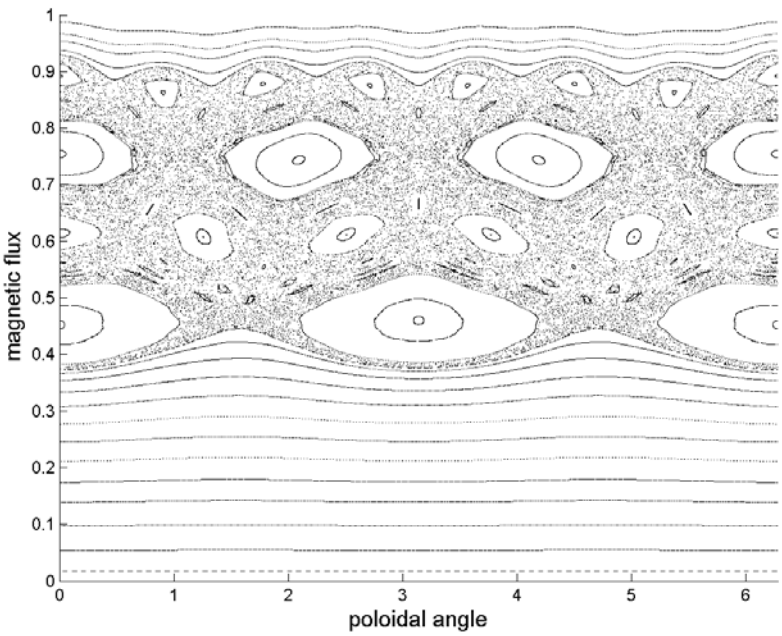

Figure 5: Chaotic orbit, when $(2,1)$, $(5,2)$, $(3,1)$ and $(7,2)$ modes are simultaneously activated

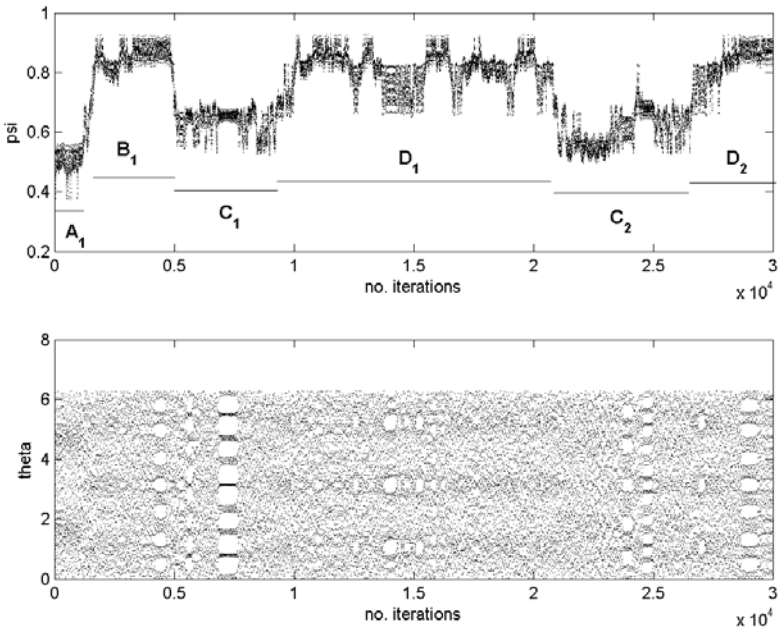

Figure 6: The variation of ψ (top) and θ (bottom) along the orbit of $(\theta_0, \psi_0) = (1.5, 0.49)$

The chaotic orbits pass through destroyed KAM barriers and surround all islands (Figure 6). This fact becomes evident if we look the variation of ψ. The orbit starts near the hyperbolic point of $(2, 1)$ type, it encircles the chain of two islands (zone A_1 in Figure 6) then it jumps near the $(7, 2)$ mode and moves around the islands (zone B_1 in Figure 6). It spend some time around $(5, 2)$ mode (zone C_1 in Figure 6), then it oscillated between the $(7, 2)$ and $(3, 1)$ modes (zone D_1 in Figure 6). It comes back near $(5, 2)$ mode (zone C_2 in Figure 6), moves back near $(7, 2)$ and $(3, 1)$ modes (zone D_2 in Figure 6) and so on.

The distribution of θ (bottom in figure 6) shows that the points of the orbits are uniformly spread in the poloidal section. In some zones, for example in the middle of zone C_1 one can observe some "steps"(a thin zone appears in the corresponding part of Figure 6, top). It means that the points of the orbits are very close to the hyperbolic points (of type $(8, 3)$ which are situated between $(5, 2)$ and $(3, 1)$ island chains, in our example). The sojourn times near various modes are different and non-uniformly distributed along the orbit.

There are not transport barriers inside the chaotic zone.

In order to study the formation of the transport barriers, we observe that the MHD-model is a twist system, because the winding function (11) is monotonous. In this case it results from KAM theory [17] that the internal transport barriers are invariant curves (corresponding to invariant surfaces in tokamak) which can not be crossed by the magnetic field lines. A rigorous study of the formation/destruction of transport barrier, based on Aubray-Mather theory [18] or on Greene's criterion [19], is impossible in our case, due to the complicate form of the MHD-map, whose values are obtained numerically (when the implicit equations are numerically solved). For this reason we will use a numerical experiment based on the computation of the transmissivity [20].

First of all we must observe that a transport barrier can be built by decreasing the magnetic perturbations' amplitudes (in this case the stable unstable manifolds of different modes do not overlap) or by modifying the safety factor in order to create a low shear

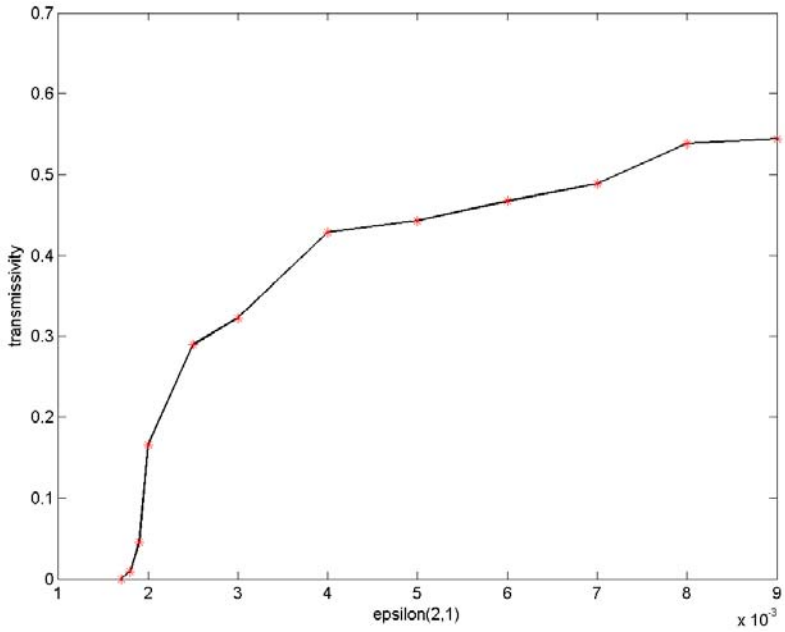

Figure 7: The transmissivity for $\varepsilon_{5,2} = 0.001$, $\varepsilon_{3,1} = 0.002$, $\varepsilon_{7,2} = 0.0005$ and various values of $\varepsilon_{2,1}$

zone (in this case the map which generate the system is close to an integrable one).

In the present study we focus on the modification of the magnetic perturbations. We consider $\varepsilon_{5,2} = 0.001$, $\varepsilon_{3,1} = 0.002$ respectively $\varepsilon_{7,2} = 0.0005$ to be the amplitudes of the perturbations corresponding to $(5, 2)$, $(3, 1)$ and $(7, 2)$ modes (as in figure 5 and we vary $\varepsilon_{2,1}$.

In order to observe the existence of a transport barrier between $(2, 1)$ and $(5, 2)$ modes and to investigate the diffusion across the barrier after its break-up we compute the transmissivity [20], defined as the fraction of orbits of fixed length, starting from the line $\psi = \psi_{2,1}$, which arrive in the vicinity of $(5, 2)$ mode.

In order to compute the transmissivity, we placed $N = 62800$ equally distanced initial conditions on the line $\psi = \psi_{2,1} = 0.456311$, and we considered their orbits of length $L = 10^4$. An orbit arrives in the vicinity of $(5, 2)$ mode when it crosses the line $\psi_{5,2} = 0.610635$. The main results are presented in figure 7. The abscises of the red stars represent the values of $\varepsilon_{2,1}$ for which the transmissivity was computed, the black line corresponds to data's linear interpolation.

We conclude that a transport barrier exists between $(2, 1)$ and $(5, 2)$ modes when $\varepsilon_{2,1} = 0.0018$ because $TR\,(0.0018) = 0$.

This barrier is just broken for $\varepsilon_{2,1} = 0.0019$ because the transmissivity $TR\,(0.0019) = 0.0094$ is strictly positive but small (just a few orbits cross the broken barrier). When $\varepsilon_{2,1}$ increases, the gaps in the broken barrier become larger, more and more orbits traverse it and the transmissivity increases.

5 Conclusions

Realistic models to the study the turbulence of magnetic configurations in tokamaks can be obtained using MHD-perturbations. In such models, the chaotic behavior is explained by the overlaps of stable and unstable manifolds of various modes, when they are simultaneously activated. We studied the destruction of a transport barrier using the transmissivity between the chaotic zones situated on its two sides. We obtained numerically the values of the perturbations' amplitudes for which the barrier is broken.

References

[1] del Castillo-Negrete, D. & Morrison, P. J. [1993], Chaotic transport created by rossby waves in shear flow, Phys. Fluid A 5, 948-965.

[2] Rypina, I., M.G.Brown, Beron-Vera, F. J., Kocak, H., Olascoaga, M. J. & Udovydchenkov, I. [2007] , On the lagrangian dynamics of atmospheric zonal jets and the permeability of the stratospheric polar vortex, Journal of the Atmospheric Sciences 64, 3595-3610.

[3] Smirnov, I. P., Virovlyansky, A. L. & Zaslavsky, G. M. [2001], Theory and applications of ray chaos to underwater acoustics, Phys. Rev. E 64, 036221.

[4] Munteanu, A., Petrisor, E., Garcia-Berro, E. & Jose, J. [2003], Creation of twistless circles in a model of stellar pulsations," Communications in Nonlinear Science and Numerical Simulation 8, 355-373.

[5] Balescu, R. [1998],Hamiltonian nontwist map for magnetic field lines with locally reversed shear in toroidal geometry, Phys. Rev. E 58, 3781-3792.

[6] Balescu, R., Vlad, M. and Spineanu, F. [1998], Tokamap: a hamiltonian twist map for magnetic field lines in a toroidal geometry, Phys. Rev. E 58, 951-964.

[7] Morrison, P. J. [2000], Magnetic field lines, hamiltonian dynamics, and nontwist systems, Physics of Plasmas 7, 2279-2289.

[8] E. Hairer, C. Lubich, G.Wanner, Geometric numerical integration, Springer Verlag Berlin Heidelberg, 2002

[9] S. S. Abdulaev, On mapping models of field lines in a stochastic magnetic field, Nuclear Fusion 44 (2004) S12-S27

[10] Dubois M. A., Sabot R., Pegourie B., Drawin H.-W. Geraud A., Determination of the safety factor profile in Tore-Supra from the largest striations observed during the pellet ablation, Nuclear Fusion, vol 32, no.11,1992, 1935-1940

[11] Misguich J. H. , Reuss J. D., Weysow B., D.Constantinescu, Steinbrecher G.,Balescu R., M. Vlad, Spineanu F., Noble internal transport barriers and radial subdiffusion of toroidal magnetic lines,Annales de Physique 28 (2003) N°6, pp. 1-101

[12] V. Igochine, O. Dumbrajs, D. Constantinescu, H. Zohm, G. Zvejnieks and the SDEX Upgrade Team, Stochastization as a possible cause for fast reconnection during MHD mode activity in the ASDEX Upgrade tokamak, Nucl. Fusion 46 (2006) 741–751

[13] Abdullaev S.S., Generic magnetic field model in poloidal divertor tokamaks in the presence of magnetic perturbations, Nuclear Fusion 50(2010) 034001

[14] Meskat J. P., Zohm H., Gantenbein G., Gunter S., Maraschek M., Suttrop W, Yu Q. and ASDEX Upgrade Team, Analysis of the structure of the neoclassical tearing modes in ASDEX-Upgrade, Plasma Phys. Controlled Fusion 43 (2001), 1325

[15] Abdulaev S.S., Model of a magnetic field in poloidal divertor tokamaks affected by resonant magnetic perturbations, Physics of Plasmas 16 (2009), 030701

[16] Abdullaev S.S., Universal asymptotics of poloidal spectra of magnetic perturbations of saddle coils in tokamaks, Physics of Plasmas 18 (2011), 020701

[17] Moser J., Stable and random motion in dynamical systems, Princeton University Press, 1973

[18] Mather J.N., Existence of quasi-periodic orbits for twist homeomorphisms of the annulus, Topology 21 no.4 (1982) 457-467

[19] Greene J., A method for determining a stochastic transition, J. Math Phys 20 (1979) 1183-1201

[20] Szezech Jr. J.D., Caldas I. L., Lopes S. R., Viana R. L., Morrison P. J., Transport properties in nontwist area-preserving maps, Chaos 19 (2009), 043108